Current Research in Food Science 6 (2023) 100408

Contents lists available at ScienceDirect

Current Research in Food Science

journal homepage: www.sciencedirect.com/journal/current-research-in-food-science

Preparation process optimization and evaluation of bioactive peptides from *Carya cathayensis* Sarg meal

Fujie Yan [a], Qingqing Wang [b], Jialuo Teng [a], Fenghua Wu [b], Zhiping He [b,c,*]

[a] Department of Food Science and Nutrition, College of Biosystems Engineering and Food Science, Zhejiang University, Hangzhou, 310058, China
[b] College of Food and Health, Zhejiang Agriculture and Forest University, Hangzhou, 311300, Zhejiang, China
[c] College of Food Science and Engineering, Xinjiang Institute of Technology Xinjiang, Aksu, 843100, China

ARTICLE INFO

Keywords:
Antioxidant peptide
Carya cathayensis Sarg meal
Protein hydrolysate
Physicochemical characteristics
Cytoprotective effect
Caenorhabditis elegans

ABSTRACT

Carya cathayensis Sarg meal (CM) is a by-product of the edible kernel during oil manufacture. In order to improve wastes utilization, the CM derived peptides (CMPs) that showed an *in vitro* radical scavenging ability were firstly prepared by five different hydrolases. Alcalase treatment revealed the highest yield and the optimal conditions were further determined by response surface methodology (RSM), under which the yield reached 35.84%. Simulated gastrointestinal digestion led to an enrichment of low molecular weight (MW) peptides (<3 kDa), which was beneficial for protecting hepatocyte damaged by hydrogen peroxide (H_2O_2). Furthermore, generated hydrolysates exhibited protective effects on paraquat-induced *Caenorhabditis elegans* via enhancing expressions of Skinhead-1 (SKN-1) and its downstream target including glutathione S-transferase (GST)-4 and superoxide dismutase (SOD)-3 to diminish oxidative stress. Taken together, our results demonstrated that simple enzymatic hydrolysis of crude protein powder from CM represents an efficient, eco-friendly and economical strategy for producing bioactive peptides, which can be supplemented in nutraceutical products and food preservation.

1. Introduction

Oxidative stress is caused by the imbalance between reactive oxygen species (ROS) production and elimination, resulting in a series of physiological and pathological reactions (Sies, 2017; Forman and Zhang, 2021). The development of antioxidant peptides is one of the research hotspots in the field of antioxidant. In comparison with proteins, peptides have attracted the attention of scholars at home and abroad due to their lower molecular weight, easier absorption, low economic cost and good safety (Deng et al., 2021; Durand et al., 2021). Natural peptides can be used as nutritional supplements and natural antioxidants in the treatment of oxidative stress. The potential mechanisms of antioxidant peptides are as follows: (1) scavenge free radicals; (2) chelate metal ions; (3) inhibition of lipid peroxidation; (4) activate cellular antioxidant defense system (Wen et al., 2020). There are various studies about production, purification and identification of antioxidant peptides (Agrawal et al., 2019; Q. Zhang et al., 2019). The preparation of bioactive peptides by enzymatic hydrolysis is preferred because this technique is easily controlled and with no residual organic solvents or toxic chemicals in the product (Beaubier et al., 2019).

Carya cathayensis Sarg (Chinese hickory) is a deciduous perennial fruit tree belonging to Juglandaceae family. It is a high-quality dry fruit and woody oil crop peculiar to China, mainly produced in Zhejiang and Anhui provinces (Yang et al., 2015). The edible part of Chinese hickory is the nuts and its protein content is about 20% which contained all human essential amino acid. Additionally, the kernel contains abundant kinds of mineral elements in hickory nuts, especially for calcium, potassium, zinc that is far more than general dry nuts (He et al., 2012). Compared with walnut and pecan, Chinese hickory kernel has a higher nutritional value, being loved by customers due to its unique taste and intellectual benefits. Hickory kernel oil is rich in unsaturated fatty acids, which has been reported to have antioxidant effects both *in vitro* and *in vivo* experiments. Due to the high nutritional value, more and more businesses are focus on the production of hickory oil. It has been showed that the level of triacylglycerol reduced in rat fed high-fat diets after ingested a certain amount of pecan (*Carya illinoinensis*) oil (Domínguez-Avila et al., 2015). Nevertheless, the hickory cake after being pressed is generally discarded as waste, which can cause environmental pollution and health problems. After defatted, Chinese hickory kernel still contains a lot of bioactive ingredients such as protein, which can improve the added value if reasonable being utilization. Given protein derived from hickory nut meal contains rich arginine, glutamic acid and

* Corresponding author. College of Food and Health, Zhejiang Agriculture and Forest University, Hangzhou, 311300, Zhejiang, China.
E-mail address: hzp@zafu.edu.cn (Z. He).

https://doi.org/10.1016/j.crfs.2022.100408
Received 13 September 2022; Received in revised form 24 November 2022; Accepted 30 November 2022
Available online 5 December 2022

aspartic acid that is beneficial for human health, it is a good candidate for bioactive peptides production. In the food and pharmaceutical industry, preparation of bioactive peptides by enzymatic hydrolysis is a kind of optimization method. Using such a technology not only improve the functional properties and biological characteristics of proteins, but also improve commercial values of relevant products. To the best of our knowledge, for hickory by-products, most of researches concentrated on polyphenol extraction from leaves, peels and shells (Xiang et al., 2016; Kureck et al., 2018; Fu et al., 2021, 2022; Tang et al., 2021), few about peptides processing. The preparation of peptides from CM can make more effective use of Chinese pecan protein resources as well as improve the added value of Chinese pecan, being a new breakthrough point to extend the Chinese pecan industry chain.

Here, in order to promote the high-value utilization of *C. cathayensis*, we aimed to obtain CMPs by enzymatic hydrolysis, and optimize processing conditions to increase yields by RSM. Furthermore, we evaluated their physicochemical characteristics followed by explore their biological activity through *in vitro* and *in vivo* antioxidant experiments. Our research will provide theoretical basis for the reuse of by-products and the development of antioxidant peptide food.

2. Materials and methods

2.1. Materials and reagents

Chinese pecans were obtained from Lin'an Tongda Food Co., Ltd. (Hangzhou, China), which were harvested in late September 2021. And the CM was obtained from the local farm market of Hangzhou, after Chinese pecans being oil extraction. 2′,7′-dichlorofluorescin diacetate (DCFH-DA), and dihydroethidium (DHE) were obtained from Sigma-Aldrich (St. Louis, MO, U.S.A.). 5,5‘,6,6’-Tetrachloro-1,1‘,3,3’-tetraethylbenzimidazolylcarbocyanine iodide (JC-1) was obtained from Yeasen (Shanghai, China). Naphthalene-2,3-di-carboxal-dehyde (NDA) was obtained from Life Technologies. 3-(4,5-Dimethyl-2-thiazolyl)-2,5-diphenyl-2Htetrazolium bromide (MTT), methyl viologen dichloride were purchased from Aladdin (Shanghai, China). All other reagents were of analytical grade.

2.2. Preparation of protein powders

Crude protein was obtained by the alkaline extraction and acid precipitation method according to the previous research with small modification (Zhu et al., 2019). Briefly, the defatted meal was put in solution (the ratio for material and liquid is 1:16, 1000 U/g alkaline protease) with pH 10 adjusted by 0.5 M NaOH for 1.5 h at 50 °C. After centrifugation, supernatants were adjusted to pH 3.7 with 0.5 M HCl and centrifugated at 7000 r/min, 4 °C for 20 min after standing for 2 h. After washing precipitates by distilled water, the protein powder was obtained by freeze-drying, and preserved at −20 °C.

2.3. Enzymatic hydrolysis

Enzymatic hydrolysis of the CM was performed with five different enzymes at indicated conditions (Table S1). Hydrolysis was stopped by heating at 95 °C for 15 min to inactivate the enzymes. The insoluble material was removed by centrifugation at 7000 r/min, 4 °C for 20 min, supernatants were stored at −80 °C overnight and water was removed by lyophilization. Peptides powder was kept at −20 °C for further experiments.

2.4. Yield of peptide calculation

2.5 mL 10% trichloroacetic acid solution was added to 2.5 mL enzymolysis solution, followed by shaking and mixing for 10 min, and centrifugation at 7000 r/min for 10 min. After centrifugation, the supernatant was transferred to a 10 mL volumetric flask, and the volume was fixed with 5% trichloroacetic acid solution. After homogenization, 1 mL solution was absorbed into a 10 mL volumetric flask with pipette, and the volume was diluted with 5% trichloroacetic acid solution. 6 mL of the above diluted enzymatic hydrolysate was taken and 4 mL of biuret reagent was added. After the shaking was uniform, it was placed at 25 °C for 30 min, and then the absorbance value was measured at the wavelength of 540 nm.

2.5. Fourier transform infrared spectroscopy (FTIR) and X-ray diffraction

The secondary structure of the protein powder and CMP1 was determined by FTIR spectroscopy. The detection was carried out under the conditions of resolution of 4 cm^{-1} and wave number of 4000-400 cm^{-1} by KBr pressing. PeakFit V4.12 software was used to perform the second derivative and deconvolution curve fitting analysis.

The X-ray diffraction spectrum of the protein powder and CMP1 was analyzed on an X-ray diffractometer, which recorded the spectra in the angle range of 5°–90° (2θ).

2.6. Amino acid analysis

The five kinds of CMPs were hydrolyzed in 6.0 M HCl at 150 °C for 2 h. And the amino acid composition of the hydrolysates after derivatization were examined with High Performance Liquid Chromatograph (HPLC). The standard mixed 17 kinds of amino acid were treated as the same method described above (Zhao and Zhang, 2020).

2.7. Process of in vitro digestion

10 mg CMPs were dissolved in saline and HCl was used for adjusting pH to 2. After adding 1% pepsin, the mixture was reacted at 37 °C for 90 min. When the gastric digestion ended, $NaHCO_3$ was added to adjust pH to 7.4, samples supplemented with 0.3% bile salts and 1% trypsin were reacted at 37 °C for another 3 h. Reactants were heated at 95 °C for 15 min and then centrifugated at 12000 r/min, 4 °C for 20 min to remove precipitation.

2.8. MW distribution assay

The molecular weight range of the five CMPs was determined by HPLC. Samples were separated using gel chromatography column $TSKgelG2000SW_{XL}$ (7.8 mm× 300 mm) as a flow rate of 0.5 mL/min, with the column temperature at 30 °C and UV detection wavelength at 220 nm. Consist of mobile phase is 10% acetonitrile and 0.1% trifluoroacetic acid. Cytochrome C (MW 12384 Da), aprotinin (MW 6511 Da), insulin (MW 5807 Da), Gly-Gly-Try-Arg (MW 451 Da) and Gly-Gly-Gly (MW 189 Da) were used as standard molecular weight markers.

2.9. Determination of in vitro antioxidant activities

The determination of DPPH radicals scavenging ability was analyzed according to a modified measurement of previous study (Ai et al., 2022). Briefly, 500 μL of peptides (5 mg/mL) were mixed with 500 μL of freshly prepared DPPH solution (0.2 mM in methanol) and allowed to react at room temperature in the dark. Sterile phosphate buffer saline (PBS) was taken as blank samples. After 30 min of reaction, the samples were centrifuged at 7000*g* for 10 min and the supernatant was taken to × measure the absorbance at 517 nm (A_{517}).

$$\text{DPPH inhibition } (\%) = [A_{517}\ (\text{sample})\ / A_{517}\ (\text{blank})] \times 100\%$$

ABTS radical cation ($ABTS^{\cdot+}$) was produced by reacting 10 mL of 7 mM ABTS (98%, Aladdin, China) with 179 μL of 140 mM $K_2S_2O_8$ for 14 h in the dark at room temperature. It was diluted 20 times with distilled water before use. 500 μL of peptides (5 mg/mL) and 500 μL of $ABTS^{\cdot+}$ solution were mixed and incubated for 6 min in the dark at room temperature. Sterile PBS was taken as blank samples. The samples were

centrifuged at 7000×*g* for 10 min and the supernatant was taken to measure the absorbance at 734 nm (A_{734}).

$$\text{ABTS inhibition}\ (\%) = [1 - A_{734}\ (\text{sample})\ /\ A_{734}\ (\text{blank})] \times 100\%$$

FRAP assay was performed following a modified method according to (Ai et al., 2022). FRAP reagent was prepared by mixing 300 mM NaAc buffer (pH 3.5), 10 mM 2,4,6-Tris(2-pyridyl)-s-triazine (TPTZ), and 20 mM $FeCl_3$ $6H_2O$ in the ratio of 10:1:1 (*V/V/V*). 500 μL samples were mixed with 500 μL of FRAP reagent and incubated in the dark at 37 °C for 30 min. The samples were centrifuged at 7000×*g* for 10 min and the supernatant was taken to measure the absorbance at 593 nm. The reducing ability of strains was expressed by equivalent Vitamin C (Vc).

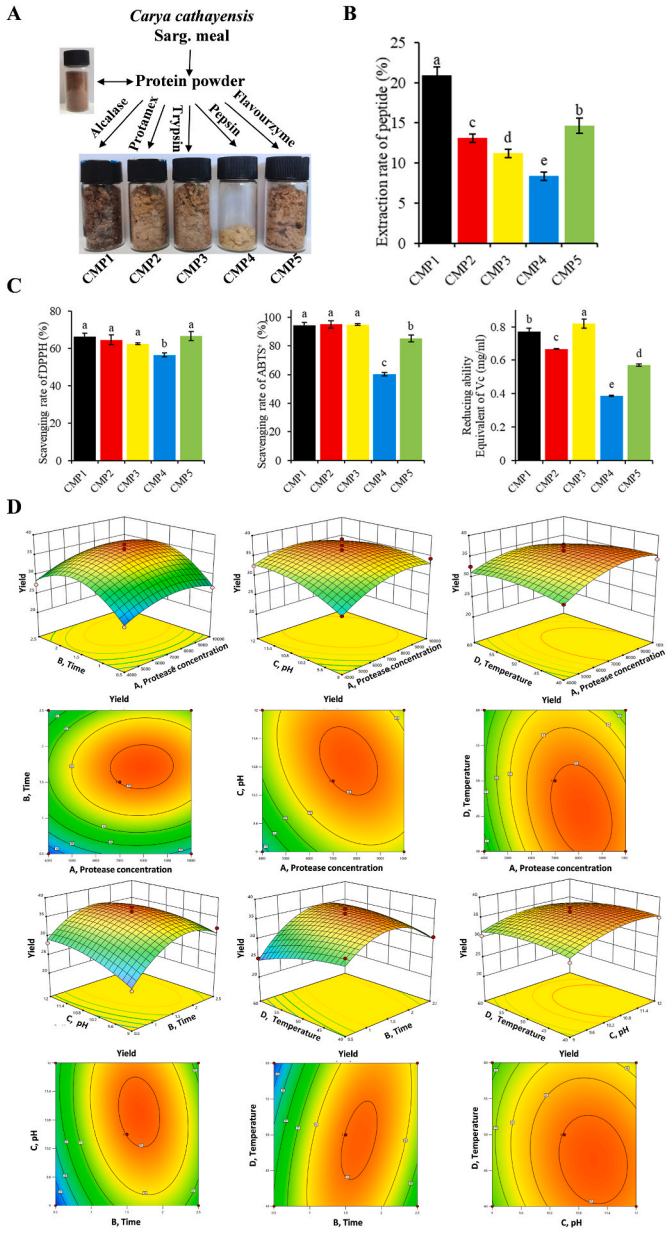

Fig. 1. Peptides preparation and corresponding antioxidant capacities. (A) Flow chart of the preparation process for the five kinds of hydrolysates and their appearance pictures. (B) The peptide yield of CM by various proteases. All data were expressed as mean values (mean ± SD, n = 3). Different letters indicate a significant difference ($P < 0.05$). (C) The *in vitro* antioxidant activities of CMPs are evaluated by DPPH radical scavenging ability, ABTS radical scavenging activity and FRAP assay, separately. The data are presented as mean ± SD, for three independent experiments. Values indicated by the bars with different letters are significantly different ($P < 0.05$, one-way ANOVA). (D) The 3D surfaces (the first and third rows) and contour plots (the second and fourth rows) of responses for yield. Four factors of protease concentration (A), temperature (B), pH (C) and time (D) are compared in pairs. Twelve figures showed the result of the pairwise comparison, corresponding to Table 1.

2.10. Cell culture

Human normal hepatocyte L02 (Human liver-7702) cell line was obtained from the Cell Bank of Type Culture Collection of Chinese Academy of Sciences. Cells were cultured in RPMI 1640 medium with 10% fetal bovine serum and 100 units/mL each of penicillin and streptomycin at 37 °C under 5% CO_2.

2.11. Cell viability assay

Cell viability was determined by the MTT assay (Yan et al., 2017a,b). L02 cells were seeded into 96-well cell culture plates at the density of 1 × 10^4 cells/well and incubated for 24 h. After incubation, the cells were treated with 50, 100 and 200 μg/mL of CMP1 for 24 h, followed by exposure to 0.4 mM H_2O_2 for a further 6 h. Subsequently, the cells were washed twice with PBS and incubated with 0.5 mg/mL MTT for 4 h. Finally, dimethyl sulfoxide (DMSO) was added to each well to dissolve the formazan precipitate. The optical density was measured at 490 nm by a microplate reader in triplicate (Tecan, Switzerland).

2.12. Determination of ROS, superoxide anion radicals (O_2^-) and MMP

Cellular ROS was detected by the transmission of non-fluorescent DCFH-DA to fluorescent 2′,7′-dichlorofluorescein (DCF). In brief, L02 cells were incubated in 24-well cell culture plates at a density of 6 × 10^4 cells/well for 24 h. Then, the cells were treated with 50 μg/mL CMP1 for 24 h, then incubated with 0.4 mM H_2O_2 for 6 h. After treatments, the cells were washed with PBS and incubated with DCFH-DA (10 μM) for 30 min, then washed with PBS again, and evaluated immediately by a fluorescence microscope. Cellular O_2^- production was analyzed using a DHE probe. L02 cells were subjected to the same treatment procedure illustrated as the ROS measurement.

JC-1 fluorescent probes were used to determine the intracellular MMP. In brief, L02 cells were incubated in 24-well cell culture plates at a density of 6 × 10^4 cells/well for 24 h. Then, the cells were treated with 50 μg/mL CMP1 for 24 h and incubated with 0.4 mM H_2O_2 for 6 h. After above treatments, the cells were washed with PBS and incubated with JC-1 (6 μg/mL) for 30 min, then washed with PBS again, and evaluated immediately by a fluorescence microscope.

The results were calculated by Image-Pro Plus 6.0 (Media Cybernetics, Inc., Singapore) and expressed as the mean fluorescence intensity.

2.13. Measurement of intracellular glutathione (GSH)

Cells with different treatments were digested with trypsin and incubated with 50 μM NDA (for GSH labelling) for 30 min. After washing with PBS three times, cells were immediately evaluated by flow cytometer. The results from flow cytometer were analyzed by Flow Jo. On the other hand, lysates of cells were obtained using Western/IP Lysis Buffer (Beyotime, China) and reduced GSH levels measured with the corresponding commercial Kit (Nanjing Jincheng, China).

2.14. Anti-oxidation and ageing experiments in C. elegans

2.14.1. Maintenance, synchronization and treatments

Worms were cultured in nematode growth medium (NGM) plates (3 g/L NaCl, 2.5 g/L peptone, 17 g/L agar, 25 mM potassium phosphate, 1 mM $CaCl_2$ $.2H_2O$, 1 mM $MgSO_4$ $.7H_2O$, and 12.9 mM cholesterol) containing *Escherichia coli* OP50 as food at 22 °C (Cao et al., 2019). When most of worms were grown in the stage of L4 larvae, they were collected

with M9 buffer (42.25 mM Na_2HPO_4, 1 mM $MgSO_4$, 22.06 mM KH_2PO_4, 85.56 mM NaCl) and lysed to obtain eggs via synchronization. As for the treatment, synchronized worms were exposed to paraquat (1 mM) with/without CMP1 (0.1, 0.2 and 0.5 mg/mL) or GSH (0.5 mM) except for the control group. Indicators including motility and corresponding fluorescence intensities were measured after 72 h exposure.

2.14.2. Lifespan assay

Synchronized young adult worms were grown in NGM with 5-fluoro-2′-deoxy-β-uridine (5-FudR, 50 μg/mL) and OP50 containing different agents during the whole life span. A total of 30–40 young adults were cultured on each NGM and worms were counted every other day. Nematodes were transferred to new plates with indicated substances every 5 days. Worms that did not move when gently touched with a platinum wire were considered dead. The whole experiments were repeated three times (Yan et al., 2017a,b).

2.14.3. Movement assays

Synchronous nematodes (L4-stage) were transferred to NGM plates with different treatments. On the 3rd day, nematodes were inspected using a stereomicroscope. The movement of one wavelength of the nematode relative to the long axis of its body was recorded as body bending. The head of a nematode can swing from side to side, so recovery was considered as a head swing. The number of body bends is counted within 60 s and head swing times is counted within 20 s, with no less than 30 nematodes in each group.

2.14.4. O_2^- production in N2 nematodes

On the 3rd day of adulthood with indicated treatments, worms were washed three times with M9 buffer and exposed to 100 μL probe dyes for 3 h. O_2^- production were measured by DHE (10 μM). Then nematodes were washed, stiffened and randomly selected to measure the fluorescence intensity by a fluorescence microscopy at the same exposure time. At least 30 nematodes in each group were analyzed, and images were analyzed using the Image-Pro Plus 6.0 software.

2.14.5. Expressions of skn-1, gst-4 and sod-3

Strains of LD1 [*skn-1b/c*::GFP], VP596 [*gst-4p*::GFP::NLS] and CF1553 [*sod-3p*::GFP] were used for this assay. Twenty randomly selected worms after indicated treatments were transferred to slides containing M9 buffer with 0.2% levamisole and was captured with a fluorescence microscope and each experiment was performed in triplicate. The fluorescence was quantified using Image-Pro Plus 6.0 software.

2.15. Statistical analysis

All data are expressed as the mean ± standard deviation (SD) from three independent experiments. One-way ANOVA analysis with a post hoc multiple range significant difference (Duncan) test was performed to determine statistical significance ($P < 0.05$) using SPSS 22.0.

3. Results and discussion

3.1. Preparation of peptides and corresponding productivity

As shown in Fig. 1A, the color of five kinds of powders is significantly different: CMP1 is close to dark brown, colors of CMP2, CMP3 and CMP5 are similar that are shallower than CMP1, and CMP4 is close to medium yellow. The enzymatic hydrolysis effect of different proteases is obviously different due to the substrate specificity of proteases. The results showed that the order of peptide yield was alcalase > flavourzyme > protamex > trypsin > pepsin (Fig. 1B). Therefore, we thought alkaline protease is a good candidate for CMPs production. Alcalase is regarded a "serine endopeptidase" that provides information about the catalytic structure of the classical amino acid catalytic triad, of which serine is one (Tacias-Pascacio et al., 2020). Ahmadifard et al. (2016) illustrated that Alcalase presented a better degree hydrolysis of rice bran protein and soy-been protein in comparison with papain and a kind of commercial enzymes named cocktail. For Atlantic sea cucumber, alcalase-produced hydrolysates involved higher degree of hydrolysis than trypsin-produced ones (Zhang et al., 2020). We speculated that Alcalase caused the highest yield due to the extensive recognized range of amino acids, and Alcalase also trends to give a hydrolysate with smaller molecular weight. Besides, the hydrophobic amino acids on the protein side of carboxyl and aromatic amino acids with strong specificity and can release more amino acids and peptides with antioxidant capacity. Industrial food-grade proteases mainly include animal protease, plant protease and microbial protease, which have been widely used in the preparation of antioxidant peptides. For example, pepsin and trypsin have been used to prepare antioxidant peptides from tuna, salmon, cobia and so on (Yang et al., 2008; Nazeer et al., 2011). The ultrasonic effect can destroy the aggregation state of protein, so that the protein can be more evenly distributed in the liquid. It has been reported that the ultrasound treatment could affect the protein structure so that increase susceptibility of substrates to proteolysis, leading to antioxidant activities improvement (Wen et al., 2018, 2019). Microbial fermentation is also considered as a cost-effective technology to convert proteins into bioactive peptides (Abd Rashid et al., 2022). In this regard, in order to increase the output and improve the biological activity, combination of other technologies with enzymatic hydrolyzation may be a potential strategy for CMPs production.

3.2. Amino acid composition and antioxidant activity in vitro

As shown in Table S2, no significant difference of amino acid composition among five hydrolysates. Acid amino acids including aspartic acid and glutamic acid were the most abundant amino acid in the enzymolysis products, accounted for 35% of total samples. CMPs are also rich in arginine that is a kind of alkaline amino acid, which exceed more than 10%. Many previous studies have shown that one of the most important factors affecting antioxidant peptides is the amino acid composition of peptides. The side chain charged groups on acidic and alkaline amino acids can chelate metal ions and form a complex, which is considered to have certain antioxidant capacity (Chen et al., 1995; Najafian and Babji, 2018). Such amino acids ensure good antioxidant activities of CMPs including DPPH free radical scavenging capacity. At the concentration of 5 mg/mL, DPPH scavenging capacity of five CMPs was 66.3%, 64.6%, 62.5%, 56.4% and 66.5%, respectively (Fig. 1C). Results of ABTS clearance rate presented similar trends, and concrete values were higher, reaching 94.2%, 94.9%, 94.8%, 60.2% and 85.3%, respectively. Additionally, CMP3 had the highest Fe^{2+} chelating ability of 0.82 mg/mL equivalent of Vc, followed by CMP1 and CMP2 (Fig. 1C). Among them, CMP4 showed the lowest antioxidative activities, implying pepsin was not suitable for producing antioxidative peptides here. Different exposure degree of side chain groups among CMPs may lead to distinct abilities although amino acid composition is similar, explaining results we obtained. Moreover, Zhang et al. (2022) obtained CM-derived peptides by ultrafiltration and gel filtration chromatography, and found that the substances with MW lower than 3 kDa have the highest antioxidant capacity. Six peptides were next identified including FYSLHTF, VLFSNY, SSGHTLPAGV, VYGYADK, TFQGPPHG, YTPEYQTK. VYGYADK and VLFSNY could combine with key amino acid residues of a transcription factor Kelch like ECH-associated protein 1 (Keap1) through molecular docking, partly explaining their stronger antioxidant capacities. Combining our results with existing studies, we thought that CMPs are promising candidates for other novel bioactive peptides discovery. It is meaningful to further separation and purification of such hydrolysates by technologies of ultrafiltration, reversed phase high performance liquid chromatography, size-exclusion chromatography, iron-exchange chromatography and so on.

Table 1
Results of regression model and analysis of variance (ANOVA) based on peptide yield.

Source	Squares	DF	Mean Square	P Value
Model	360.92	14	25.78	<0.0001***
A	28.12	1	28.12	0.0012**
B	58.17	1	58.17	<0.0001***
C	22.61	1	22.61	0.0027**
D	4.37	1	4.37	0.1322
AB	0.5329	1	0.5329	0.5854
AC	7.56	1	7.56	0.0540
AD	3.71	1	3.71	0.1630
BC	5.66	1	5.66	0.0901
BD	20.98	1	20.98	0.0035**
CD	0.7310	1	0.7310	0.5237
A^2	44.19	1	44.19	0.0002***
B^2	188.54	1	188.54	<0.0001***
C^2	22.99	1	22.99	0.0025**
D^2	8.23	1	8.23	0.0456*
Residual	23.93	14	1.71	
Lack of Fit	19.90	10	1.99	0.2675
Pure Error	4.03	4	1.01	
Cor Total	384.85	28		
$R^2 = 0.9378$				
$R^2_{adj} = 0.8757$				
cv = 4.15				

DF, degree of freedom; Significant, *p < 0.05; Very significant, **p < 0.01; Extremely significant, ***p < 0.001.

3.3. Optimization of enzymolysis technology conditions by RSM

Based on the results of peptides yield and antioxidant activity, we chose alcalase as the hydrolase for further process optimization. Parameters including enzyme concentration (A), hydrolysis time (B), pH value (C) and temperature (D) were designed for the preparation of peptides, and the experimental responses were shown in Table S3. Levels of four factors were A (4000, 7000 and 10000 U/g), B (0.5, 1.5 and 2.5 h), C (9, 10.5 and 12) and D (40, 50 and 60 °C), respectively. In addition, all the significant parameters were retained after the ANOVA test running. The regression coefficients and statistical parameters for dependent variables are presented in Table 1. Fig. 1D showed the influence and interaction of four factors on the peptides yield. The following formula showed the yield of the peptide (Y) as a function of A, B, C and D by applying multiple regression analyses to experimental data.

$$Y = +36.04 + 1.53A + 2.20B + 1.37C - 0.6033D + 0.3650AB - 1.38AC - 0.9625AD - 1.19BC + 2.29BD - 0.4275CD - 2.61A^2 - 5.39B^2 - 1.88C^2 - 1.13D^2$$

The higher values of the R^2 (0.9378), R^2_{adj} (0.8757) and CV (4.15) advocated the model as highly significant. The P values of linear coefficients (A, B and C), quadratic term coefficients (A^2, B^2, C^2 and D^2) and interaction coefficients (BD) were below 0.05, indicating that it was significant for the effects of these items on protein extraction yield from CM residues. Compared with the P values of the monomial variance, the

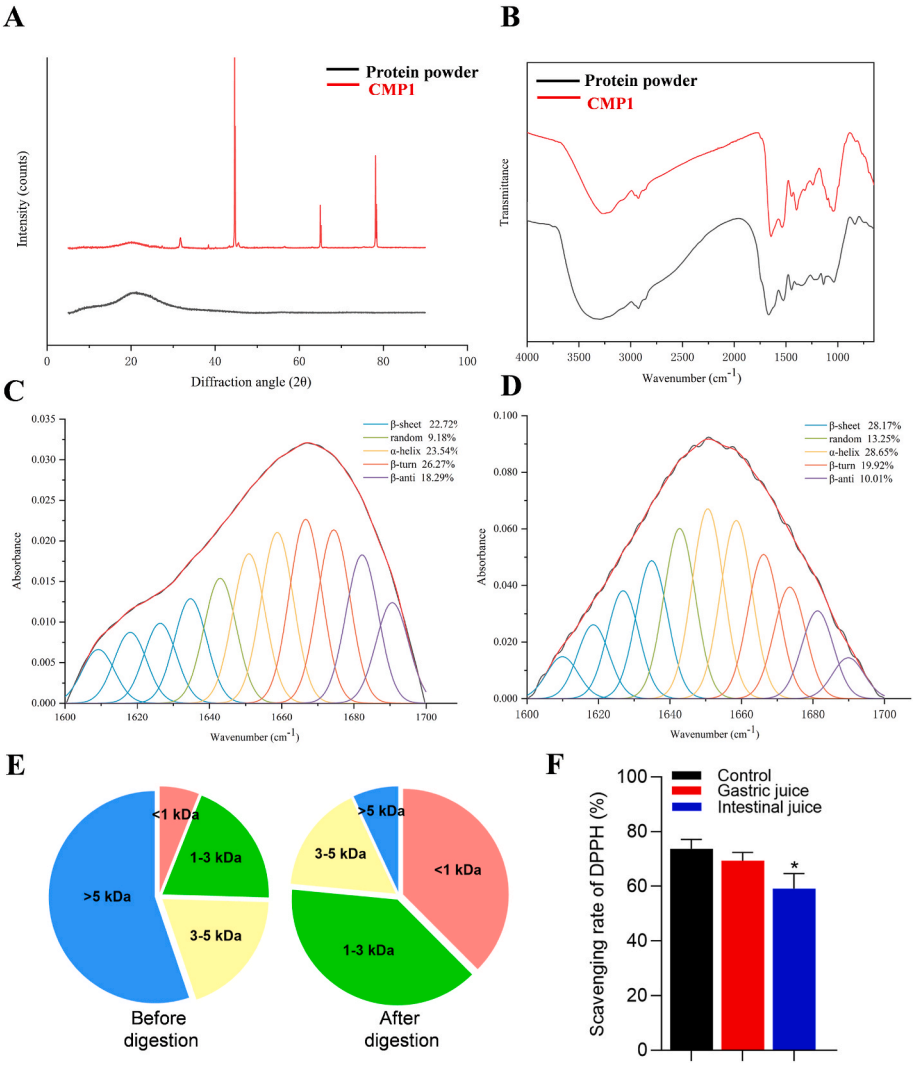

Fig. 2. Physicochemical characteristics alteration of protein powder after hydrolyzed by alcalase. (A) X-ray diffraction curves; (B) FTIR spectra; Deconvolution and curve-fitting of FTIR spectra of amide I bands for the protein powder (C) and CMP1 (D). (E) Molecular weight range alteration of CMP1 after simulated gastrointestinal digestion. (F) DPPH radical scavenging activity of CMP1 after digested by gastric juice and intestinal juice. *P < 0.05 represents significant difference compared with the control group.

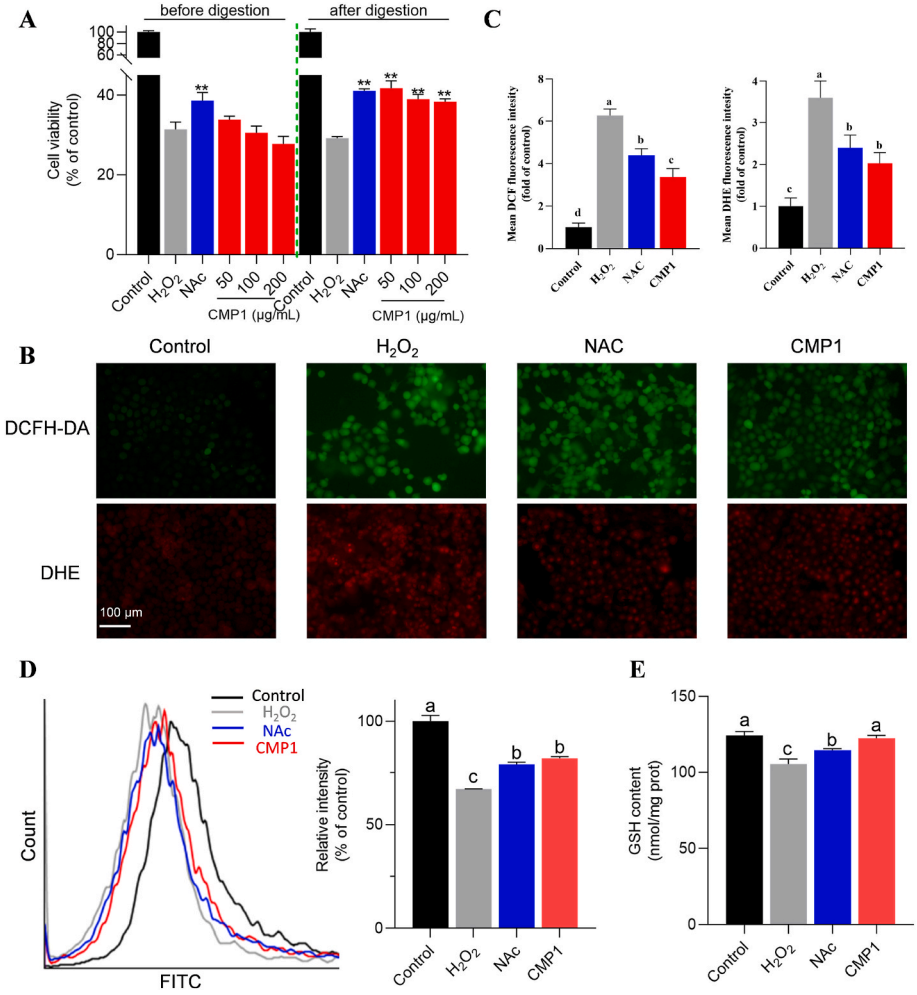

Fig. 3. Antioxidative ability change of CMP1 after *in vitro* digestion. (A) Protective effect of CMP1 (before/after *in vitro* digestion) on H_2O_2-induced cytotoxicity. The cell viability was measured by the MTT assay. $^{**}P < 0.01$ represents highly significant difference compared with H_2O_2-treated group. (B) Effects of CMP1 on H_2O_2-induced ROS and superoxide anion radical generation measured by 10 μM DCFH-DA or DHE fluorescent probe. (C) shows the quantitative data of panel. (D) Flow cytometry analysis of GSH content detected by NDA fluorescent. Left, histogram of flow cytometry; Right, relative fluorescence intensity compared with the control group. (E) Reduced GSH content detected by the commercial kit. Values indicated by the bars with different letters are significantly different ($P < 0.05$, one-way ANOVA).

effect order of relevant factors on the protein extraction yield was as follow: hydrolysis time (B) > enzyme concentration (A) > pH value (C) > temperature (D). Verification test was performed to check on the accuracy of the proposed model. Taking the actual operation in the experiment into account, the predicted values were adjusted: enzyme concentration, 7881.84 U/g; time, 1.62 h; pH 10.89 and temperature, 46.77 °C. Under this condition, the actual yield of CMP1 was 35.84% that was much higher than the initial yield (21%) and slightly lower than the predicted value (36.66%) obtained by the regression, demonstrating that the model fitted well with the actual situation.

3.4. Fourier infrared spectroscopy and X-ray diffraction

For the protein powder, there was no obvious diffraction peak observed, indicating a poor crystallinity. While the characteristic diffraction peaks of CMP1 appear at 44.7°, 65° and 78.14°, suggesting that enzymatic hydrolysate leads to remarkable changes in crystallinity (Fig. 2A). Results of FTIR spectra revealed the structural differences between the original protein powder and CMP1, especially in the range from 1600 to 1700 cm^{-1} that represent the secondary structure characteristics (Fig. 2B). Further analysis at this wavenumber coverage showed that CMP1 contains larger amounts of β-sheet, random and α-helix but a smaller amount of β-turn, compared with the original protein powder (Fig. 2C and D).

3.5. Alteration of antioxidant activity and molecular weight range after simulated gastrointestinal digestion

More than half of the MW of the direct enzymatic hydrolysate is larger than 5 kDa, while *in vitro* simulated gastrointestinal digestion led to an enrichment of low molecular weight peptides (Fig. 2E). MW is an important factor affecting the antioxidant capacity of peptides, and many scholars believe that MW is negatively correlated with antioxidant capacity, that is, the smaller the molecular weight is, the higher the antioxidant activity of peptides. The steric hinders caused by the reaction of large peptides with free radicals make it difficult for the active site to bind to free radicals. We firstly want to increase the utilization of by-products and yield is the only response factor. However, excessive peptide yield may not be able to obtain peptides with a strong antioxidant capacity even result in less bioactivity (You et al., 2009). Fortunately, CMP1 under the condition after optimization exhibited 73% clearance rate of DPPH radical, which was similar with the level before (Figs. 1C and 2F). Moreover, gastric juice digestion did not change DPPH scavenging ability while the scavenging ability of free radicals was decreased in the digestive part of intestinal fluid (Fig. 2F). Our studies showed that smaller molecular weight polypeptides do not have the stronger *in vitro* antioxidant activity, suggesting the sequence and composition of amino acids may also affect their antioxidant activity.

3.6. CMP1 pretreatment rescues H_2O_2-induced cytotoxicity and oxidative damage in L02 cells

Oxidative damage is a common pathophysiological basis of liver

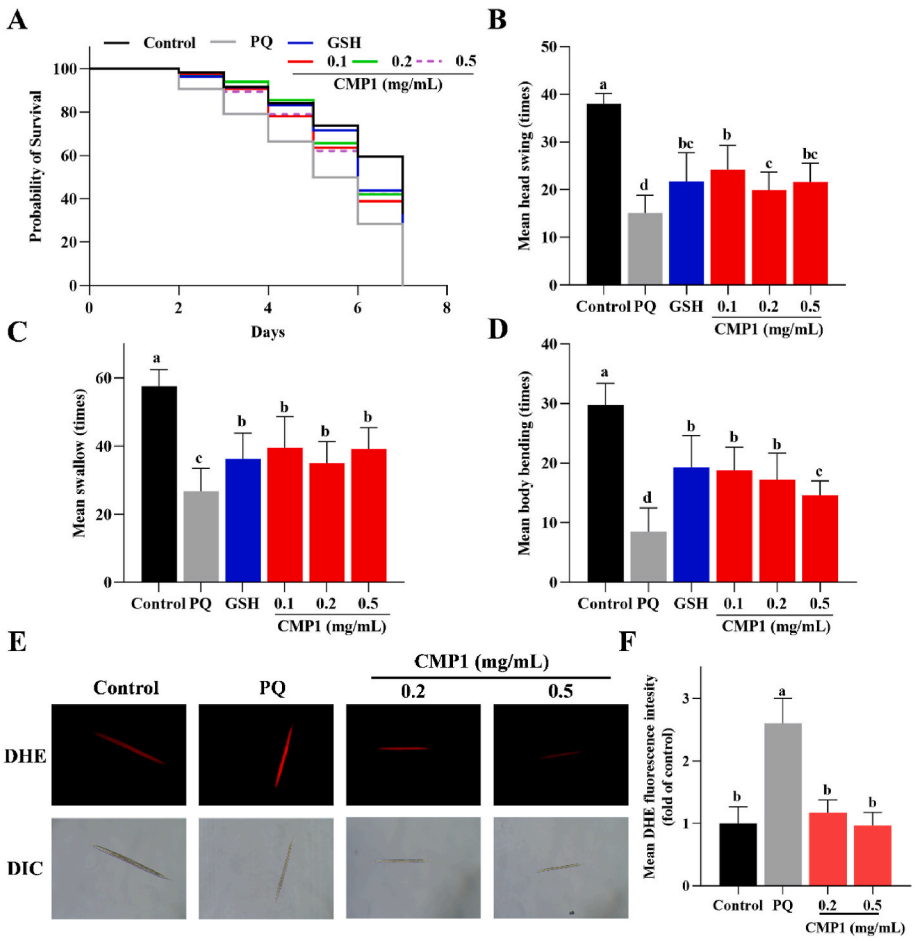

Fig. 4. Effects of CMP1 on paraquat-induced physiological toxicity in *C. elegans*. (A) Lifespan assay on worms with different treatments. (B–D) The impact of CMP1 intervention on head swing times (1 min), pharyngeal pumping rate (20 s) and body bending times (20 s) of worms. (E) O_2^- generation detected by DHE probe. (F) shows the quantitative data of panel. DIC, shapes of strains under normal light field; PQ, paraquat. Values indicated by the bars with different letters are significantly different ($P < 0.05$, one-way ANOVA).

injury and L02 cell line has been regarded as a fine model for antioxidants evaluation at a cellular level. For example, Wang et al. (2018) indicated that diosmetin restores notable injury to L02 cells treated by H_2O_2 and Ma et al. (2022) found gamma-oryzanol exerts the cytoprotective effects in H_2O_2-induced L02 cell apoptosis. Similarly, in the present study, we observed that the L02 cell viability was significantly decreased after exposure to H_2O_2 (0.4 mM) for 6 h, the survival rate was reduced to 31.36% in comparison to untreated cells, indicating a successful establishment of the oxidative damage model. As seen from Fig. 3A, direct hydrolysates had no obvious protective effect on H_2O_2-exposed cells. However, cells pretreated with such hydrolysates that after *in vitro* digestion, showing higher survival rates than that of oxidation injury group. CMP1 at the concentration of 50 μg/mL revealed the best cytoprotection which was equal to N-Acetyl-L-cysteine (NAC, a precursor of GSH), a kind of common antioxidant that is often used as a positive control (Y. Zhang et al., 2019; Jing et al., 2022; Li et al., 2022). Enhancing the dose of CMP1 didn't improve the protective effect (Fig. 3A). Combing with the results of CMP1 MW distribution, MWs of most peptides before digestion are higher than 3 kDa that occupy 75%, which is hard for cells utilization. After digestion, smaller peptides are more easily absorbed by the intestinal mucosa and react with free radicals, explaining the discrepancy between DPPH eliminating ability and cellular protective effect of CMP1. Simulated gastrointestinal fluid digestion further hydrolyzes CMP1 into smaller molecules, leading to better cellular absorption and utilization.

Considering the yield and antioxidative activity, we chose digested CMP1 for further investigation. A sharp increase of ROS levels can cause serious damage to cellular structures and function. A significant increase of ROS accumulation was detected in H_2O_2-treated L02 cells (6-fold of control) according to the mean DCF fluorescence intensity (Fig. 3B and C). This effect was strikingly inhibited by pretreatment with CMP1 and the mean fluorescence intensity was decreased to 3.2-fold of the control. Furthermore, DHE was used to determine the cellular level of the superoxide anion radical, which could also cause oxidative damage. Consistently, similar results were obtained and displayed in Fig. 3B and C. The mean DHE fluorescence intensity was plunged to 1.8-fold of the control in the presence of 50 μg/mL CMP1 compared to solely H_2O_2 treatment (3.5-fold of the control). These results collectively manifested that CMP1 could suppress H_2O_2-induced ROS accumulation in L02 cells.

Since GSH is capable of scavenging intracellular ROS, we further determined the GSH content by a fluorescence probe NDA. As shown in Fig. 3E and F, H_2O_2 led to a GSH depletion in L02 cells, which could be effectively reversed by both 2 mM NAC and CMP1 pretreatments. Mitochondria are a major source of oxidants and a target for their damaging effects. Besides, mitochondrial membrane potential (MMP) is the prerequisite for maintaining mitochondrial oxidative phosphorylation and adenosine triphosphate production, and the stability of MMP is conducive to maintaining normal physiological functions of cells. In this study, the JC-1 fluorescent probe was used to detect the effect of CMP1 on keeping MMP balance in L02 cells suffered H_2O_2 injury. Cells without suffering oxidative stress injury had a very low intensity of green fluorescence. When suffered 0.4 mM H_2O_2 for 6 h, the rate of red/green decreased 60% compared with the control, while CMP1 pretreatment could partly restore this reduction (Figs. S1A and B). Continuous mitochondrial oxidative stress accumulation eventually leads to loss of mitochondrial function, such as reduced mitochondrial oxidative phosphorylation, inefficient electron transport and further increased oxidant flux (Cogliati et al., 2016). For L02 cells, CMP1 had beneficial effects on inhibiting cellular ROS generation and improving GSH levels, clearly suggesting that CMP1 could act as an antioxidant targeted to

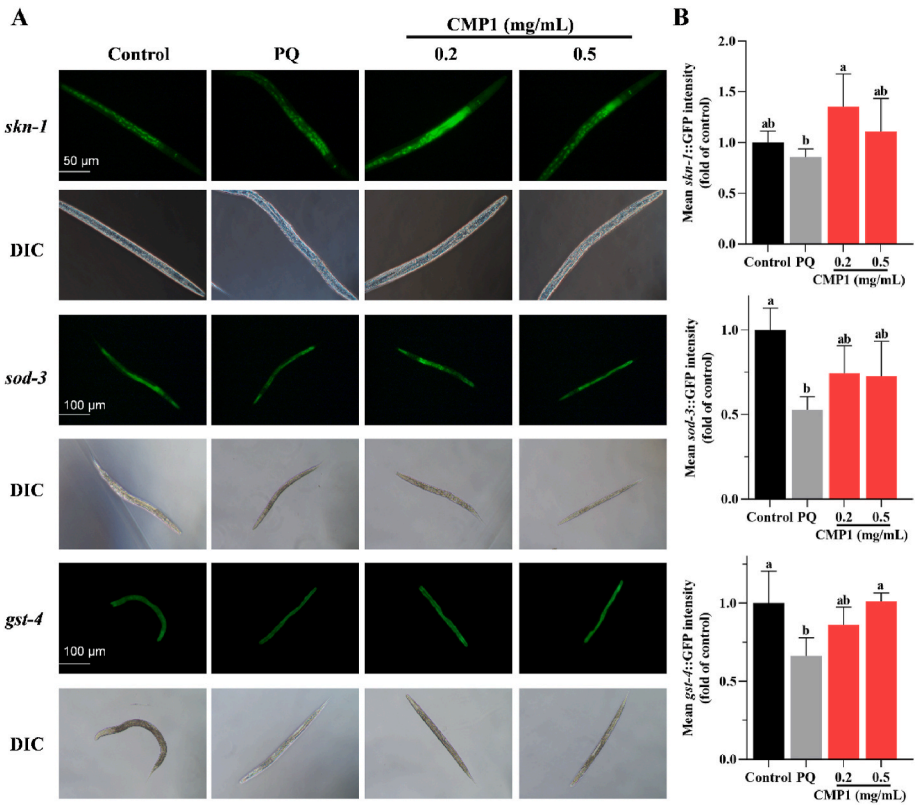

Fig. 5. Effects of CMP1 on paraquat-induced oxidative damage in *C. elegans*. (A) Levels of GFP-targeted *skn-1*, *sod-3* and *gst-4* expressions in transgenic LD1, CF1553 and VP596 strains. (B) shows the quantitative data of panel. DIC, shapes of strains under normal light field; PQ, paraquat. Values indicated by the bars with different letters are significantly different ($P < 0.05$, one-way ANOVA).

mitochondria to suppress hepatic oxidative damage.

3.7. CMP1 attenuates paraquat induced toxicity and oxidative stress in C. elegans

C. elegans has become a classic model organism in the field of aging research because of its clear genetic background, simple structure, short life cycle and easy culture (Calvo et al., 2016). Here, we take *C. elegans* as the research model to explore the effects of CMP1 on oxidative damage remission *in vivo*. Paraquat can act as an electron acceptor, acting on the redox reaction of cells and activating into oxygen free radicals in cells, resulting in lipid peroxidation of cell membranes and oxidative damage (Dilberger et al., 2019a; Bora et al., 2021). Many studies have used paraquat to study the response of *C. elegans* to oxidative stress (Dilberger et al., 2019b; Lu et al., 2021). The survival rate of worms barely exposed to paraquat (1 mM) apparently decreased, all worms died while the control groups maintained a 60% survival rate at day 7. Intervention with CMP1 could effectively improve the survival rate, 32%, 38%, 40% survival rate was observed at 7th day when worms suppled with CMP1 at concentrations of 0.1, 0.2 and 0.5 mg/mL (Fig. 4A). Similar results also observed in other indicators like head swing times within 1 min, body bending times and swallow times within 20 s, respectively (Fig. 4B–D). Taken above data together, we suggested that CMP1 could also moderate paraquat induced toxicity in N2 *C. elegans*.

In L02 cells, CMP1 rescued H_2O_2 induced oxidative stress. Likewise, we explored oxidative stress related indicators of O_2^- generation using DHE probes in paraquat-treated *C. elegans* and results were consistent with that found in L02 cells. Generally, in comparison with the control group, the DHE fluorescence intensity of paraquat-treated group were dramatically increased while CMP1 suppressed this increase (Fig. 4E and F). In *C. elegans*, SKN-1transcription factor that is an ortholog of NF-E2-related factor 2 (Nrf2) in human, playing an important role in oxidative stress amelioration, and regulating downstream genes such as *gst-4* and *sod-3* to extend lifespan (Li et al., 2019; Song et al., 2020). SOD is an antioxidant metal enzyme existing in organisms, which can catalyze the superoxide anion radical disproportionation to generate oxygen and hydrogen peroxide, and plays a crucial role in the balance between oxidation and antioxidant. GST-4 is associated with glutathione metabolism and biosynthesis (Pohl et al., 2019). Levels of SKN-1, SOD-3 and GST-4 in worms were impaired by paraquat, implying more free radical production couldn't be timely removed. Supplementation of CMP1 led to a slight increase of proteins expressions mentioned above compared with paraquat-treated group (Fig. 5A and B). Therefore, we consider that CMP1 protected *C. elegans* against paraquat induced oxidative stress and SKN-1 might be a potential target.

4. Conclusions

In this work, we demonstrated that simple alkaline protease hydrolyzation is a good strategy for peptides production from CM residues due to its highest yield and bioactivity. RSM was used to gain the optimal parameter of CMP1 processing (7881.84 U/g enzyme concentration, 46.7 °C, pH 10.89 and 1.62 h) and the final yield reached 35.84%. Further digestion by gastric and intestinal juices makes CMP1 hydrolyze into smaller molecules, which is beneficial for cell utilization. The result of cellular experiments showed that CMP1 after digestion has the capacity to alleviate cytotoxicity induced by H_2O_2 in hepatic cells, which subsequently results in excessive free radicals scavenging and GSH contents recovery. *In vivo* studies, we presented evidence that CMP1 also extends the lifespan of *C. elegans* by eliminating oxidative stress. The research on the preparation of bioactive peptides from CM can make a better use of by-products after oil pressing and provide new technical support for comprehensive development and deep processing of *C. cathayensis*, improving the economic value. Additionally, further

isolation, purification and identification of antioxidative peptides from CMP1 is worthwhile to obtain novel bioactive peptides with definite amino acid sequences.

CRediT authorship contribution statement

Fujie Yan: Conceptualization, Methodology, Investigation, Writing – original draft. **Qingqing Wang:** Data curation, Visualization. **Jialuo Teng:** Data curation. **Fenghua Wu:** Methodology, Supervision. **Zhiping He:** Funding acquisition, Validation, Writing – review & editing.

Declaration of competing interest

The authors declare that they have no known competing financial interests or personal relationships that could have appeared to influence the work reported in this paper.

Data availability

The data that has been used is confidential.

Acknowledgements

This work was supported by grants from the cooperation projects between the People's Government of Zhejiang Province and the Chinese Academy of Forestry (2019SY04), the Zhejiang Provincial Key R&D Program of China (No. 2020C02040) and Natural Science Foundation of Xinjiang Uygur Autonomous Region (2021D01A71).

Appendix A. Supplementary data

Supplementary data to this article can be found online at https://doi.org/10.1016/j.crfs.2022.100408.

References

Abd Rashid, N.Y., Manan, M.A., Pa'Ee, K.F., Saari, N., Faizal Wong, F.W., 2022. Evaluation of antioxidant and antibacterial activities of fish protein hydrolysate produced from Malaysian fish sausage (*Keropok Lekor*) by-products by indigenous *Lactobacillus casei* fermentation. J. Clean. Prod. 347, 131303.

Agrawal, H., Joshi, R., Gupta, M., 2019. Purification, identification and characterization of two novel antioxidant peptides from finger millet (*Eleusine coracana*) protein hydrolysate. Food Res. Int. 120, 697–707.

Ahmadifard, N., Murueta, J.H.C., Abedian-Kenari, A., Motamedzadegan, A., Jamali, H., 2016. Comparison the effect of three commercial enzymes for enzymatic hydrolysis of two substrates (rice bran protein concentrate and soy-been protein) with SDS-PAGE. J. Food Sci. Technol. 53, 1279–1284.

Ai, F., Huang, X., Wu, Y., Ji, C., Gao, Y., Yu, T., Yan, F., 2022. Alleviative effects of a novel strain *Bacillus coagulans* XY2 on copper-induced toxicity in zebrafish larvae. J. Environ. Sci. 125, 750–760.

Beaubier, S., Framboisier, X., Ioannou, I., Galet, O., Kapel, R., 2019. Simultaneous quantification of the degree of hydrolysis, protein conversion rate and mean molar weight of peptides released in the course of enzymatic proteolysis. J. Chromatogr. B 1105, 1–9.

Bora, S., Vardhan, G.S.H., Deka, N., Khataniar, L., Gogoi, D., Baruah, A., 2021. Paraquat exposure over generation affects lifespan and reproduction through mitochondrial disruption in *C. elegans*. Toxicology 447, 152632.

Calvo, D.R., Martorell, P., Genovés, S., Gosálbez, L., 2016. Development of novel functional ingredients: need for testing systems and solutions with *Caenorhabditis elegans*. Trends Food Sci. Technol. 54, 197–203.

Cao, X., Wang, X., Chen, H., Li, H., Tariq, M., Wang, C., Zhou, Y., Liu, Y., 2019. Neurotoxicity of nonylphenol exposure on *Caenorhabditis elegans* induced by reactive oxidative species and disturbance synthesis of serotonin. Environ. Pollut. 244, 947–957.

Chen, H., Muramoto, K., Yamauchi, F., 1995. Structural analysis of antioxidative peptides from soybean. Beta. - conglycinin. J. Agric. Food Chem. 43, 574–578.

Cogliati, S., Enriquez, J.A., Scorrano, L., 2016. Mitochondrial cristae: where beauty meets functionality. Trends Biochem. Sci. 41, 261–273.

Deng, Z., Yang, Z., Peng, J., 2021. Role of bioactive peptides derived from food proteins in programmed cell death to treat inflammatory diseases and cancer. Crit Rev Food Sci 1–19.

Dilberger, B., Baumanns, S., Schmitt, F., Schmiedl, T., Hardt, M., Wenzel, U., Eckert, G. P., Jadeja, R., 2019a. Mitochondrial oxidative stress impairs energy metabolism and reduces stress resistance and longevity of *C. elegans*. Oxid. Med. Cell. Longev. 2019, 6840540.

Dilberger, B., Baumanns, S., Schmitt, F., Schmiedl, T., Hardt, M., Wenzel, U., Eckert, G. P., Jadeja, R., 2019b. Mitochondrial oxidative stress impairs energy metabolism and reduces stress resistance and longevity of *C. elegans*. Oxid. Med. Cell. Longev. 2019, 6840540.

Domínguez-Avila, J.A., Alvarez-Parrilla, E., López-Díaz, J.A., Maldonado-Mendoza, I.E., Gómez-García, M.D.C., de la Rosa, L.A., 2015. The pecan nut (*Carya illinoinensis*) and its oil and polyphenolic fractions differentially modulate lipid metabolism and the antioxidant enzyme activities in rats fed high-fat diets. Food Chem. 168, 529–537.

Durand, E., Beaubier, S., Ilic, I., Fine, F., Kapel, R., Villeneuve, P., 2021. Production and antioxidant capacity of bioactive peptides from plant biomass to counteract lipid oxidation. Curr Res Food Sci 4, 365–397.

Forman, H.J., Zhang, H., 2021. Targeting oxidative stress in disease: promise and limitations of antioxidant therapy. Nat. Rev. Drug Discov. 20, 689–709.

Fu, X., Belwal, T., He, Y., Xu, Y., Li, L., Luo, Z., 2022. UPLC-Triple-TOF/MS characterization of phenolic constituents and the influence of natural deep eutectic solvents on extraction of *Carya cathayensis* Sarg. peels: composition, extraction mechanism and *in vitro* biological activities. Food Chem. 370, 131042.

Fu, X., Wang, D., Belwal, T., Xu, Y., Li, L., Luo, Z., 2021. Sonication-synergistic natural deep eutectic solvent as a green and efficient approach for extraction of phenolic compounds from peels of *Carya cathayensis* Sarg. Food Chem. 355, 129577.

He, Z.P., Fu, M.R., Mao, L.C., 2012. Changes of phenolics, condensed tannins and antioxidant activity of Chinese hickory (*Carya cathayensis* Sarg.) after different thermal processing. Asian J. Chem. 24, 1685–1688.

Jing, L., Sun, Y., Wang, J., Zhou, X., Shi, Z., 2022. Oxidative stress and endoplasmic reticulum stress contributed to hepatotoxicity of decabromodiphenyl ethane (DBDPE) in L-02 cells. Chemosphere 286, 131550.

Kureck, I., Policarpi, P.D.B., Toaldo, I.M., Maciel, M.V.D.O., Bordignon-Luiz, M.T., Barreto, P.L.M., Block, J.M., 2018. Chemical characterization and release of polyphenols from Pecan nut shell [*Carya illinoinensis* (Wangenh) C. Koch] in zein microparticles for bioactive applications. Plant Foods Hum. Nutr. 73, 137–145.

Li, H., Su, L., Su, X., Liu, X., Wang, D., Li, H., Ba, X., Zhang, Y., Lu, J., Huang, B., Li, X., 2019. Arginine methylation of SKN-1 promotes oxidative stress resistance in Caenorhabditis elegans. Redox Biol. 21, 101111.

Li, J., Ge, H., Xu, Y., Xie, J., Yan, F., Chen, W., 2022. Geniposide alleviates oxidative damage in hepatocytes through regulating miR-27b-3p/Nrf2 axis. J. Agric. Food Chem. 70, 11544–11553.

Lu, M., Mishra, A., Boschetti, C., Lin, J., Liu, Y., Huang, H., Kaminski, C.F., Huang, Z., Tunnacliffe, A., Kaminski Schierle, G.S., Morroni, F., 2021. Sea cucumber-derived peptides alleviate oxidative stress in neuroblastoma cells and improve survival in *C. elegans* exposed to neurotoxic paraquat. Oxid. Med. Cell. Longev. 2021, 8842926.

Ma, Y., Xiang, S., Jiang, W., Kong, L., Tan, Z., Liang, Z., Yuan, Z., Yi, J., Zhu, L., 2022. Gamma-oryzanol protects human liver cell (L02) from hydrogen peroxide-induced oxidative damage through regulation of the MAPK/Nrf2 signaling pathways. J. Food Biochem. 46, e14118.

Najafian, L., Babji, A.S., 2018. Fractionation and identification of novel antioxidant peptides from fermented fish (pekasam). J. Food Meas. Char. 12, 2174–2183.

Nazeer, R.A., Deeptha, R., Jaiganesh, R., Sampathkumar, N.S., Naqash, S.Y., 2011. Radical scavenging activity of seela (*Sphyraena barracuda*) and ribbon fish (*Lepturacanthus savala*) backbone protein hydrolysates. Int. J. Pept. Res. Therapeut. 17, 209.

Pohl, F., Teixeira-Castro, A., Costa, M.D., Lindsay, V., Fiúza-Fernandes, J., Goua, M., Bermano, G., Russell, W., Maciel, P., Kong Thoo Lin, P., 2019. GST-4-Dependent suppression of neurodegeneration in *C. elegans* models of Parkinson's and machado-joseph disease by rapeseed pomace extract supplementation. Front Neurosci-Switz 13.

Sies, H., 2017. Hydrogen peroxide as a central redox signaling molecule in physiological oxidative stress: oxidative eustress. Redox Biol. 11, 613–619.

Song, B., Zheng, B., Li, T., Liu, R.H., 2020. SKN-1 is involved in combination of apple peels and blueberry extracts synergistically protecting against oxidative stress in *Caenorhabditis elegans*. Food Funct. 11, 5409–5419.

Tacias-Pascacio, V.G., Morellon-Sterling, R., Siar, E., Tavano, O., Berenguer-Murcia, Á., Fernandez-Lafuente, R., 2020. Use of Alcalase in the production of bioactive peptides: a review. Int. J. Biol. Macromol. 165, 2143–2196.

Tang, S., Shi, Z., Qiao, X., Zhuang, Z., Ding, Y., Wu, Y., Ding, Z., Huang, Y., 2021. *Carya cathayensis* leaf extract attenuates ectopic fat deposition in liver, abdomen and aortic arch in ovariectomized rats fed a high-fat diet. Phytomedicine 82, 153447.

Wang, C., Liao, Y., Wang, S., Wang, D., Wu, N., Xu, Q., Jiang, W., Qiu, M., Liu, C., 2018. Cytoprotective effects of diosmetin against hydrogen peroxide-induced L02 cell oxidative damage via activation of the Nrf2-ARE signaling pathway. Mol. Med. Rep. 17, 7331–7338.

Wen, C., Zhang, J., Zhang, H., Duan, Y., Ma, H., 2019. Effects of divergent ultrasound pretreatment on the structure of watermelon seed protein and the antioxidant activity of its hydrolysates. Food Chem. 299, 125165.

Wen, C., Zhang, J., Zhang, H., Duan, Y., Ma, H., 2020. Plant protein-derived antioxidant peptides: isolation, identification, mechanism of action and application in food systems: a review. Trends Food Sci. Technol. 105, 308–322.

Wen, C., Zhang, J., Zhou, J., Duan, Y., Zhang, H., Ma, H., 2018. Effects of slit divergent ultrasound and enzymatic treatment on the structure and antioxidant activity of arrowhead protein. Ultrason. Sonochem. 49, 294–302.

Xiang, L., Wang, Y., Yi, X., Wang, X., He, X., 2016. Chemical constituent and antioxidant activity of the husk of Chinese hickory. J. Funct.Foods 23, 378–388.

Yan, F., Chen, Y., Azat, R., Zheng, X., 2017a. Mulberry anthocyanin extract ameliorates oxidative damage in HepG2 cells and prolongs the lifespan of *Caenorhabditis elegans* through MAPK and Nrf2 pathways. Oxid. Med. Cell. Longev. 1–12, 2017.

Yan, F., Yang, Y., Yu, L., Zheng, X., 2017b. Effects of c-glycosides from *Apios americana* leaves against oxidative stress during hyperglycemia through regulating Mitogen-

activated protein kinases and Nuclear factor erythroid 2-related factor 2. J. Agric. Food Chem. 65, 7457–7466.
Yang, J., Ho, H., Chu, Y., Chow, C., 2008. Characteristic and antioxidant activity of retorted gelatin hydrolysates from cobia (*Rachycentron canadum)* skin. Food Chem. 110, 128–136.
Yang, J., Zhou, F., Xiong, L., Mao, S., Hu, Y., Lu, B., 2015. Comparison of phenolic compounds, tocopherols, phytosterols and antioxidant potential in Zhejiang pecan [*Carya cathayensis*] at different stir-frying steps. LWT–Food Sci. Technol. 62, 541–548.
You, L., Zhao, M., Cui, C., Zhao, H., Yang, B., 2009. Effect of degree of hydrolysis on the antioxidant activity of loach (*Misgurnus anguillicaudatus*) protein hydrolysates. Innovat. Food Sci. Emerg. Technol. 10 (2), 235–240.
Zhang, J., Wu, S., Wang, Q., Yuan, Q., Li, Y., Reboredo-Rodríguez, P., Varela-López, A., He, Z., Wu, F., Hu, H., Liu, X., 2022. Oxidative stress amelioration of novel peptides extracted from enzymatic hydrolysates of Chinese pecan cake. Int Journal Mol Sci 23, 12086.
Zhang, Q., Tong, X., Li, Y., Wang, H., Wang, Z., Qi, B., Sui, X., Jiang, L., 2019. Purification and characterization of antioxidant peptides from alcalase-hydrolyzed Soybean (*Glycine max* L.) hydrolysate and their cytoprotective effects in human intestinal Caco-2 cells. J. Agric. Food Chem. 67, 5772–5781.
Zhang, Y., He, S., Bonneil, É., Simpson, B.K., 2020. Generation of antioxidative peptides from Atlantic sea cucumber using alcalase versus trypsin: *In vitro* activity, de novo sequencing, and in silico docking for *in vivo* function prediction. Food Chem. 306, 125581.
Zhang, Y., Wang, X., Chen, C., An, J., Shang, Y., Li, H., Xia, H., Yu, J., Wang, C., Liu, Y., Guo, S., 2019. Regulation of TBBPA-induced oxidative stress on mitochondrial apoptosis in L02 cells through the Nrf2 signaling pathway. Chemosphere 226, 463–471.
Zhao, Z., Zhang, Y., 2020. Greener degumming production of layered sericin peptides from a silkworm cocoon and their physicochemical characteristics and bioactivities *in vitro*. J. Clean. Prod. 261, 121080.
Zhu, Y., Zhao, X., Zhang, X., Liu, H., 2019. Extraction, structural and functional properties of *Haematococcus pluvialis* protein after pigment removal. Int. J. Biol. Macromol. 140, 1073–1083.